

FINGER VEIN RECOGNITION BY COMBINING GLOBAL AND LOCAL FEATURES BASED ON SVM

Kang Ryoung PARK

*Division of Electronics and Electrical Engineering
Dongguk University
26, Pildong-3 ga, Jung-gu, Seoul
Republic of Korea, 100-715
e-mail: parkgr@dongguk.edu*

Manuscript received 23 March 2009; revised 18 June 2010
Communicated by Steve J. Maybank

Abstract. Recently, biometrics such as fingerprints, faces and irises recognition have been widely used in many applications including door access control, personal authentication for computers, internet banking, automatic teller machines and border-crossing controls. Finger vein recognition uses the unique patterns of finger veins to identify individuals at a high level of accuracy. This paper proposes new algorithms for finger vein recognition. This research presents the following three advantages and contributions compared to previous works. First, we extracted local information of the finger veins based on a LBP (Local Binary Pattern) without segmenting accurate finger vein regions. Second, the global information of the finger veins based on Wavelet transform was extracted. Third, two score values by the LBP and Wavelet transform were combined by the SVM (Support Vector Machine). As experimental results, the EER (Equal Error Rate) was 0.011% and the total processing time was 98.2 ms.

Keywords: Biometrics, finger vein recognition, LBP, Wavelet transform, SVM

1 INTRODUCTION

Biometrics refers to ways of identifying people by using physical human features. There have been several kinds of biometric recognition systems such as fingerprint, face, iris, hand vein etc. However, these conventional systems have some problems

in terms of convenience and performance. In fingerprint and hand vein recognition systems, users have to touch the surface of the input sensor by their finger and hand. This can cause much inconvenience for the user and it is also possible to steal latent information from the fingerprint sensor. In addition, the condition of the finger surface (e.g. sweat, dryness) and skin distortion can cause degraded recognition accuracy. For face recognition, performance highly depends on facial expressions and illuminations, which can change. Iris recognition is most reliable in terms of accuracy, but the capturing device is expensive and can be inconvenient compared to other biometric systems.

To overcome these problems, vein patterns such as palm veins [13] and hand veins have been studied [14]. Vein recognition uses internal information from a person's body and vein patterns, which can be seen with infrared light illuminators and a camera. Also, it is difficult to steal internal patterns. However, the palm vein and hand vein recognition device is currently too large compared to fingerprint recognition systems.

So, finger vein recognition has been studied. Yanagawa's study proved that finger vein patterns could be properly used for personal identification [1]. They showed that each finger of each person has totally different vein patterns and a finger vein pattern shows as much degrees of freedom as iris patterns [1]. Miura proposed a way of extracting finger vein patterns by using repeated line tracking from various starting positions. There proved to be good extraction performance with regard to image shading [2]. These researchers used 678 finger vein images for identification, while the EER was 0.145% and the processing time was 460 ms [2]. Zhang also proposed an extraction method based on the curvelet information of the profile of finger vein images and locally interconnected structured neural networks [3]. The proposed neural networks were trained using information from true and false vein pattern regions [3]. These researchers used 3 200 finger vein images for matching while the EER was 0.128% [3]. In the most recent study, Miura showed that the thickness of finger vein patterns could differ due to varying amounts of blood in fingers under different weather conditions (shown by using 678 finger vein images with an EER of 0.0009%) [4]. Miura proposed finger vein pattern extraction based on the curvature value on a cross section of a finger vein pattern and extracted the points with high curvature values in each of four directions. This allowed extracting of a finger vein pattern even among various pattern thicknesses [4]. A commercial product has also been introduced by Hitachi [15]. All of those methods used the finger vein extraction method. However, finger vein images are not always clear, but can sometimes also show irregular shadings and highly saturated regions. Therefore, detection errors can arise when extracting accurate vein patterns. Also, the finger vein extraction step can lead to increase of processing time.

To overcome these problems, we propose a new finger vein recognition system. The proposed method used a LBP (Local Binary Pattern) method for extracting local information of finger-vein patterns. Using the LBP, recognition performance was reliable against irregular shadings and highly saturated regions. In addition, we extracted the global information of finger-vein patterns based on Wavelet transform.

Two score values by the LBP and Wavelet transform were combined by the SVM (Support Vector Machine) and the recognition accuracy was much enhanced.

2 THE PROPOSED SYSTEM

2.1 Finger Vein Capturing Device

In previous works, the finger vein capture devices were composed of infrared illuminators and a camera with an infrared light passing filter. The infrared illuminators were located on the back of the person's hand and infrared light then shone through the finger [2]. The light was captured by a camera underneath the finger [2]. The size of such device was big because the infrared illuminators were above the camera. This meant that the finger vein recognition system was difficult to use for many size-limited applications, such as mobile phones. To overcome these problems, we propose a finger vein capturing device [18].

First, we reduced the depth of the proposed device by using a slanted hot mirror positioned at 45 degrees in front of the camera, as shown in Figure 1. The hot mirror reflected infrared light while allowing visible light to pass through. Please note that the system shown in Figure 1 is only a prototype. Through size optimization of the hot mirror and the illuminator module shown in Figure 1, the size of the finger vein capturing system can be greatly reduced.

Second, we used a minimal guiding structure to allow the proposed system to be used by reducing the touching area of finger. In case of commercial finger vein recognition system [15], they require a user to touch the sensor by half area of finger. In our system, the minimal guiding structure includes a touching bar only for the finger tip and part of the backside of the finger. The touching area of finger of our system is smaller than that of the commercial system [15]. In this way, we obtain finger vein images without causing user's inconvenience, as shown in Figure 4.

2.2 Overview of Finger Vein Recognition Algorithm

An overview of our proposed algorithm is shown in Figure 2. First, we captured a finger vein image by using the proposed device. Next, we localized the finger region in the captured image by using the masks shown in Figure 5. The shape of each finger was found to be different, as shown in Figure 9. In order to normalize the captured finger vein images, the localized finger region was defined and stretched towards the X and Y axes, respectively, as shown in Figure 7. Then, the localized image was sub-sampled to 50×20 pixels by using a 3×3 pixel mosaic block. After that, we extracted the finger vein code by using the LBP, as explained in Section 2.6. Finally, the extracted finger vein code was matched with enrolled ones by calculating the Hamming distance (HD). We also extracted finger vein feature values by using Wavelet transform and calculated Euclidean distance (ED).

The calculated two distances (HD and ED) were combined by the SVM and user authentication (verification) was performed.

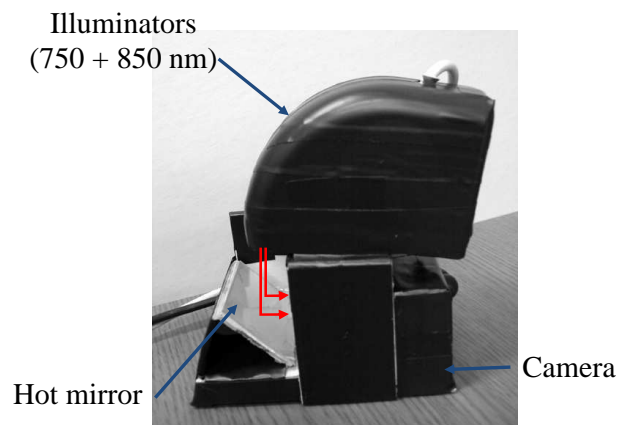


Fig. 1. Prototype of the proposed finger vein capturing device [18]

2.3 Alignment of Finger to Capturing Device

When we capture the finger vein image, there can be finger movement such as translation or rotation, as shown in Figure 3. Such movements can increase the variation of finger vein feature of authentic user, which causes the false rejection error to be increased. In order to prevent these problems, in our system the minimal guiding structure includes a touching bar only for the finger tip and for part of the

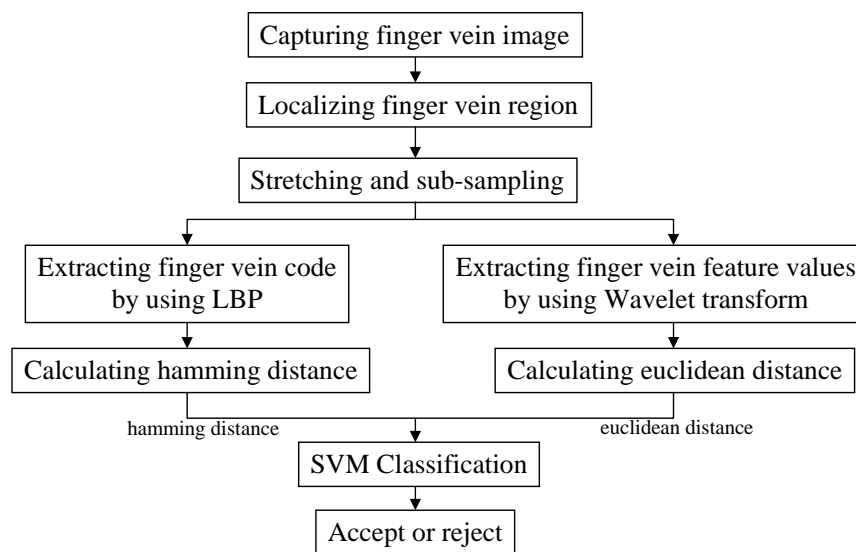


Fig. 2. Proposed finger vein recognition algorithm

backside of the finger. The touching area of finger in our system is smaller than that of the commercial system [15]. In this way, we obtain finger vein images without causing user's inconvenience, as shown in Figure 4.

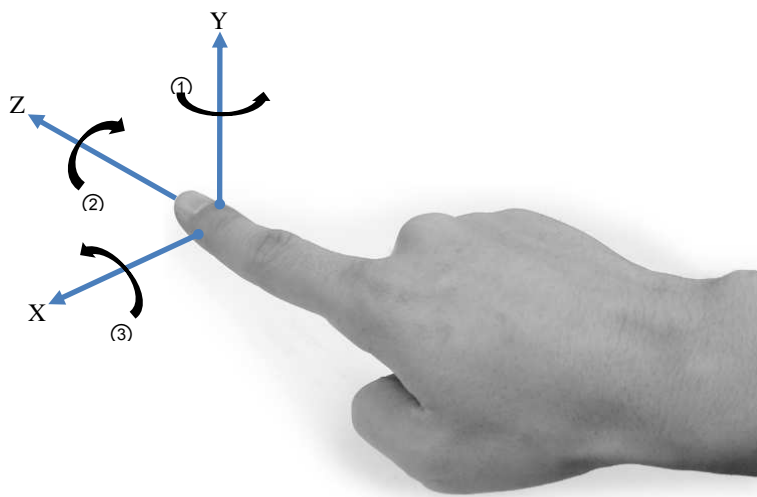


Fig. 3. Finger's movement: translation and rotation [18]



Fig. 4. Guiding structure of our system for aligning user's finger [18]

2.4 Localizing the Finger Region

The captured images included shaded regions at both ends in the horizontal direction, as shown in Figure 9. Because this caused degraded recognition, and because we were able to align the finger veins horizontally by using the guiding bar, we were easily able to cut off the shaded regions with predetermined pixel sizes at both ends.

The shapes of each person’s fingers were different, as shown in Figure 9, so we localized the finger region in order to normalize the finger vein image and extract the texture from the normalized image. The finger region is brighter than the background region, as shown in Figure 9, because infrared light shone through the skin. Therefore, in order to localize the finger region from captured images, we used the masks shown in Figures 5 a) and b). The masking value was calculated in the Y direction for each X position and the position at which the masking value became maximal was determined as the boundary position between the finger and the background in the Y direction. Figure 6 shows the result of localizing the finger region with masks.

-1	-1	-1	-1	-1	-1	-1	-1	-1	-1	-1	-1	-1	-1	-1	-1	-1	-1	-1	-1
-1	-1	-1	-1	-1	-1	-1	-1	-1	-1	-1	-1	-1	-1	-1	-1	-1	-1	-1	-1
1	1	1	1	1	1	1	1	1	1	1	1	1	1	1	1	1	1	1	1
1	1	1	1	1	1	1	1	1	1	1	1	1	1	1	1	1	1	1	1

a)

1	1	1	1	1	1	1	1	1	1	1	1	1	1	1	1	1	1	1	1
1	1	1	1	1	1	1	1	1	1	1	1	1	1	1	1	1	1	1	1
-1	-1	-1	-1	-1	-1	-1	-1	-1	-1	-1	-1	-1	-1	-1	-1	-1	-1	-1	-1
-1	-1	-1	-1	-1	-1	-1	-1	-1	-1	-1	-1	-1	-1	-1	-1	-1	-1	-1	-1

b)

Fig. 5. Masks for localizing the finer regions of the captured images [18]: a) mask for detecting the upper region of the finger; b) mask for detecting the lower region of the finger

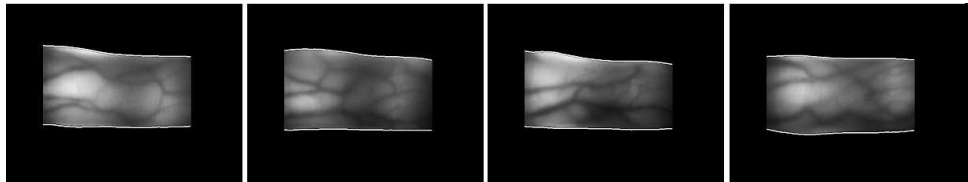


Fig. 6. Examples of localizing the finger region with masks

2.5 Stretching and Sub-Sampling the Localized Region

Then, we stretched the localized finger region in the direction of the X and Y axes. As a result, a 150×60 pixel stretched image was produced, as shown in Figure 7. Then, in order to improve processing time, the stretched image was sub-sampled to 50×20 pixels by averaging the gray values for every 3×3 pixel block.

By using sub-sampled images, the extracted finger vein features became robust against noise factors. The 3×3 pixel block was determined based on the width of the thinnest vein in the stretched image (which was measured as 3 pixels by experiment).

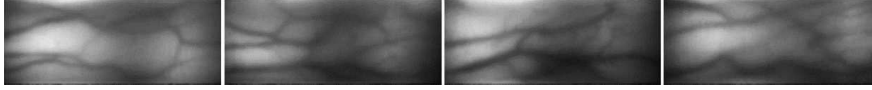


Fig. 7. Stretched images of Figure 6

2.6 Extracting the Finger Vein Code by Using the LBP: Local Features

In previous finger vein recognition [2], the method took much processing time because it was necessary to detect finger vein regions before extracting the features. So, the method had a problem that recognition performance was affected by finger vein detection errors. To overcome this problem, we used a LBP method that could extract finger vein codes in the whole vein region without requiring accurate detection of that region.

Because the LBP method compares local regions, it is robust against high saturation and irregular shadings in the captured image. The value of the LBP in the fields of face and iris recognition has been shown before [5, 6, 16]. Ojala et al. introduced the LBP operator which was a non-parametric 3×3 kernel for texture classification [8]. The LBP can be defined as an ordered set of binary values determined by comparing the gray values of a center pixel and the eight neighborhood pixels around the center, as shown in Figure 8. The ordered set of binary values can be expressed in decimal form as shown by Equation (1) [6, 18]:

$$LBP(x_c, y_c) = \sum_{n=0}^7 s(i_n - i_c)2^n, \quad (1)$$

where i_c and i_n represent the gray value of the center pixel (x_c, y_c) and the gray values of the 8 surrounding pixels, respectively [6]. The function $s(x)$ is defined as follows [6, 18]:

$$s(x) = \begin{cases} 1, & \text{if } x \geq 0 \\ 0, & \text{if } x < 0. \end{cases} \quad (2)$$

For example, if $n = 0$, $i_n = 95$ and $i_c = 112$. So, $s(i_n - i_c) = s(95 - 112) = s(-17) = 0$, $2^n = 2^0 = 1$, so, the code become 0. If $n = 1$, $i_n = 93$ and $i_c = 112$. So, $s(i_n - i_c) = s(93 - 112) = s(-19) = 0$, $2^n = 2^1 = 10$, so, the code become 00. If $n = 2$, $i_n = 95$ and $i_c = 112$. So, $s(i_n - i_c) = s(95 - 112) = s(-17) = 0$, $2^n = 2^2 = 100$, so, the code become 000. If $n = 3$, $i_n = 116$ and $i_c = 112$. So, $s(i_n - i_c) = s(116 - 112) = s(4) = 1$, $2^n = 2^3 = 1000$; so, the code becomes 1000 and so on.

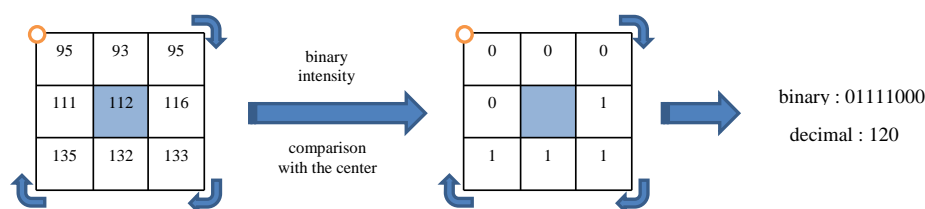


Fig. 8. The LBP operator [6]

Based on that, the proposed algorithm extracted the finger vein code into 6912 bits as 48 (the number of LBP kernel movement steps in the X direction) \times 18 (the number of LBP kernel movement steps in the Y direction) \times 8 (the number of bits per each LBP kernel) in a sub-sampled image of 50×20 pixels.

2.7 Matching the Extracted Codes With Enrolled Ones

The proposed finger vein system computed the HD to match the extracted codes with the enrolled ones. The HD is used to measure the dissimilarity between any two finger veins [7, 18], as represented as Equation (3):

$$HD = \frac{\| (codeA \otimes codeB) \cup maskA \cup maskB \|}{\| maskA \cup maskB \|}, \quad (3)$$

where \otimes is a Boolean Exclusive-OR operator between corresponding pair of bits and \cup is an OR operator. The $codeA$ and $codeB$ values are the extracted finger vein code vector and the enrolled one, respectively. The $maskA$ and $maskB$ values are the extracted control code vector and the enrolled one, respectively. The meaning of the control code vector is as follows.

The captured finger vein images include both veins and skin, as shown in Figure 9. Recognition performance is reduced by comparing the skin regions of the captured finger vein image with the skin regions of enrolled ones. Therefore, we used a control code to determine whether the extracted finger vein code was available or not. (If the code extraction position was a vein region, the control code was 1, whereas, if the code extraction position was a skin region, the control code was 0 and it was not used for recognition.) To determine the kinds of control codes of the code extraction position, we calculated the standard deviation of the 3×3 block in which LBP code was extracted. If a vein was included in the 3×3 block, the standard deviation was high because the difference between the gray values of the vein and the skin was high. If a vein was not included in the 3×3 block, the standard deviation was low because the difference between the gray values of the two skins was low. We determined the threshold of the standard deviation with which the EER (Equal Error Rate) of finger vein recognition was minimized. Experimental results showed that the threshold was 2 in our experiment.

2.8 Extracting Wavelet Transformed Features: Global Features

The finger vein code by LBP represents the local and detail features in 3×3 block. To enhance the recognition accuracy, we also extracted global features by using Wavelet transform [19]. There exist many kinds of Wavelet basis such as Haar, Gabor, Daubechies, etc. Experimental results showed that the EER of finger vein recognition was smallest in case of using Gabor basis for Wavelet transform as shown in Table 2. Optimal frequency and kernel size of Gabor bases were selected based on the minimum authentication EER (Equal Error Rate) with the training data of 2000 images (see details in Section 3).

First, we carried out multi-resolution decomposition of stretched and sub-sampled finger vein region (see Section 2.5 for the stretched and sub-sampled finger vein region) [19]. From that, defined four sub regions were defined: LL (low-frequency component in both the horizontal and vertical directions), HL (high and low-frequency component in the horizontal and vertical directions, respectively), LH (low and high-frequency component in the horizontal and vertical directions, respectively), and HH (high-frequency component in both the horizontal and vertical directions) [19, 20]. Then, each sub region was decomposed again. From that, we could obtain 16 sub regions (two-level decomposition). Then, 16 sub regions were decomposed again and we obtained 64 sub regions (three-level decomposition). From the 64 sub regions, we measured the mean and standard deviations of sub region and obtained 128 (= 64 sub regions \times 2 features) features. The number of decomposition level was determined with which minimum EER of finger vein recognition was obtained. As shown in Figure 9, because most finger vein patterns exist in horizontal direction, we assigned greater weight values to the extracted features from LH region than those from other regions. The optimal weight values were selected based on the minimum authentication EER (Equal Error Rate) with the training data of 2000 images (see details in Section 3).

Then, we calculated the Euclidean distance between the extracted 128 feature values and the enrolled ones. Because the features have continuous value, Hamming distance could not be used. By comparing the EER of finger vein recognition in case of using Euclidean distance and cosine distance, we selected the Euclidean distance which showed lower EER. Whereas the finger vein code of 6,912 bits by LBP represented local characteristics of finger vein such as detail shape of finger vein region, 128 feature values by Wavelet transform did global characteristics such as the rough shape of finger vein region.

2.9 SVM Classification

To combine the Hamming distance (HD) by LBP and the Euclidean distance (ED) by Wavelet transform, we used a SVM (Support Vector Machine). In the past, the SVM has been used to solve two class problems by determining the optimal decision hyper plane. It is based on the concept of structural risk minimization, since it measures the maximum distance to the closest points of the training set. These

measurements are known as support vectors [21]. For SVM training, we used half the images in the dataset. The other half was used for testing.

As shown in Figure 2, two distances (HD and ED) were used as the input values of the SVM. The output value of the SVM was represented as a continuous value. A value that was close to 1 represented a genuine user and a value that was close to -1 represented an imposter. The genuine means the user whose finger vein codes and features were enrolled legally. The imposter is the user whose vein code and features were not enrolled.

In order to obtain the optimal kernel for the SVM, we compared the classification performances using the RBF (Radial Basis Function), the ANOVA (ANalysis of VAriance) method, and neural, dot and polynomial kernels with the training data by using mySVM [22]. The results showed that performance when using the RBF with gamma value 100 was the best.

From the output values of SVM, we determine a genuine or imposter user based on threshold. The threshold was determined with the training data of 2 000 images. Because the outputs of SVM are categorized into two distributions such as genuine and imposter ones, we determined the optimal threshold based on conventional Bayesian rule.

3 EXPERIMENTAL RESULTS

To test our proposed finger vein recognition algorithm, we captured 10 images for each of 8 fingers (without using the thumbs of both hands) from 50 persons. Because the length of the thumb is too short to use with our capturing device, and the thumb is also difficult to use in the other commercial systems [15], we excluded the two thumbs for collecting our database. Figure 9 shows the images captured by the proposed capturing device. The database consisted of 4,000 finger vein images. The captured images were 640×480 pixels, and they were 8-bit gray images. We used a Pentium-IV 3.0 GHz processor with 1.0 GB DRAM.

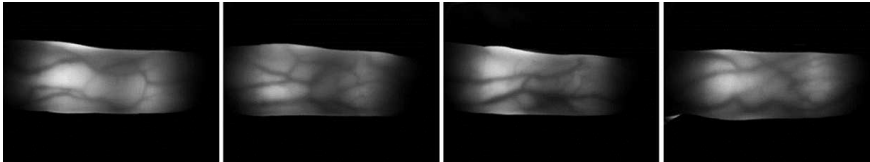


Fig. 9. Captured finger vein images of different people

In the first experiment, we tested recognition performance with finger vein images of bad quality (due to shading or saturation). First, we artificially produced bad quality finger vein images in Adobe Photoshop [17] by controlling the brightness and contrast, as shown in Figure 10. In addition, we computed the Hamming distance (HD) and Euclidean distance (ED) between the enrolled finger vein images and bad quality ones from the same user, as shown in Table 2. The HD and ED of

most images was low even though the images included shading or saturation factors. When measuring for the same user, the HD and ED was close to 0 and when for imposter users, the HD and ED was close to 1. Here, the ED was also previously normalized by the distance range of the extracted feature values.

In Table 1 and Figure 10, the HDs of the images with brightness and contrast values of -30 were higher than others. However, the main reason was the localization error, which meant that the recognition performance of the proposed method was not really affected by shading and saturation factors. In overall view, the ED was less affected by the change of brightness and contrast than the HD because it used more global features.

	Brightness	-30	-15	0	+15	+30
	Contrast	-30	-15	0	+15	+30
HD by LBP	Image 1	0.05	0.027	0.025	0.025	0.031
	Image 2	0.137	0.034	0.034	0.034	0.035
ED by Wavelet Transform	Image 1	0.03	0.022	0.021	0.022	0.024
	Image 2	0.034	0.023	0.022	0.023	0.023

Table 1. The robustness of the proposed method in terms of image shading and saturation factors

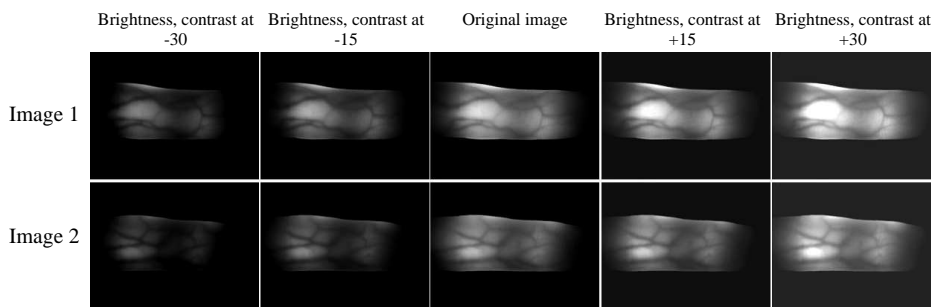


Fig. 10. Examples of artificially shaded and saturated images

In the second experiment, we tested the recognition performance. First, we measured recognition performance based on the EER and the d prime. The EER indicates the error rate when the FAR was the same as the FRR with a minimum error rate [9]. The FAR (False Acceptance Rate) means the error that occurred when an un-enrolled person was accepted as an enrolled one. The FRR (False Rejection Rate) means the error when an enrolled person was rejected as an un-enrolled one. The d prime value means the classifying ability between authentic and impostor distribution [10], defined by Equation (4)

$$d' = \frac{\mu_1 - \mu_2}{\sqrt{\frac{\sigma_1^2 + \sigma_2^2}{2}}}, \tag{4}$$

where μ_1 and μ_2 represent the means of authentic and imposter distributions, respectively, and σ_1 and σ_2 represent the standard deviations of authentic and imposter distributions. The greater the d' value was, the more separable the two distributions became and the EER became smaller [9]. The EER and d' prime of recognition are shown in Table 2.

As mentioned before, because we captured 10 images for each of 8 fingers (without using the thumbs of both hands) from 50 persons, the number of database was 4000. Because it is reported that the finger vein of each finger can be regarded as different class, the total number of classes of our database was 400 (= 8 fingers \times 50 persons). Because the proposed method requires half of data for the training of SVM, total 2000 images were used for training and the other 2000 images were used for testing. In case of "only using HD by LBP (Local Feature)" and "only using ED by Wavelet transform (Global Feature)" of Table 2, the same amount of data (2000 images) was also used for testing in order to perform fair comparisons with the proposed method.

From that, the number of authentic tests was 36000 (= 200 classes \times 9 images \times 10 times (= the enrolled image in each class was changed ten times among "10" images in order to increase the number of authentic test compared to that of imposter test) \times 2 times (we changed the group of training and that of testing, respectively)).

The number of imposter tests was 716400 (= 9 \times 199 \times 200 \times 2 times). In the number of imposter tests, "9" means that based on one enrolled image in one class, there exist 9 imposter comparisons in one different class (excluding one enrolled image among 10 images). Except for one class of enrolled images, there exist "399" classes among 400 classes, and we can change the class of enrolled image "400" times from 400 classes. "2" times means that we changed the group of training and that of testing, respectively.

		d'	EER (%)
Only using HD by LBP (Local Feature) [18]		6.913	0.029
Only using ED by Wavelet transform (Global Feature)	Haar Wavelet	4.883	0.071
	Daubechies Wavelet	5.003	0.065
	Gabor Wavelet	5.128	0.056
Proposed method (Combining Local and Global feature by SVM as shown in Figure 2)		7.487	0.011

Table 2. The accuracy of fingervein recognition

Figure 11 shows the examples of false rejection cases. Figure 11 a) represents the enrolled image. Figures 11 b) and c) show the test ones, respectively. Figure 11 b) was the case that the input finger was much misaligned by translation in the Z direction of Figure 3. Figure 11 c) was the case that much of finger rotation (along Z axis of Figure 3) happened. Although we used the shifting & matching scheme of finger vein code and features [18], false rejection happened in such cases. To overcome such problems, we plan to pre-align the finger vein image based on the

detected finger vein region and minutia points such as bifurcation and ending points of finger vein lines.

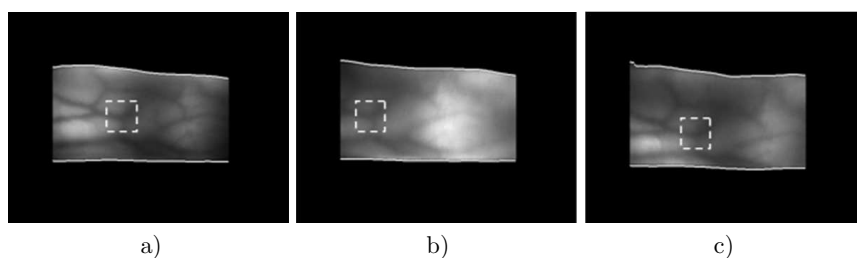


Fig. 11. Examples of false rejection cases: a) the enrolled image, b) the false rejected case 1, c) the false rejected cases 2

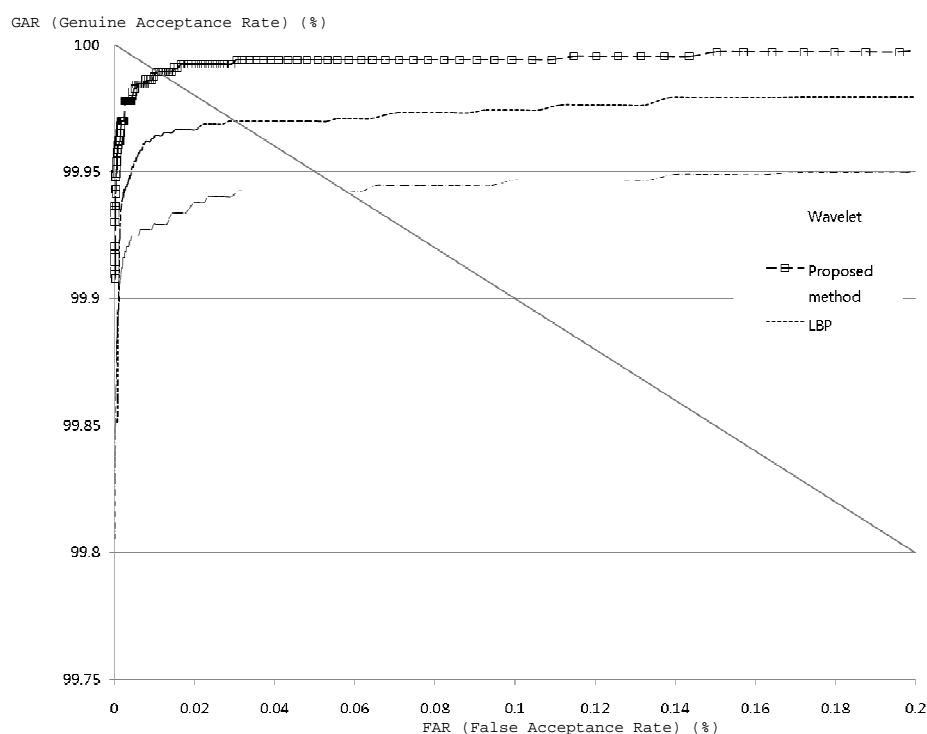


Fig. 12. ROC curve

We measured the ROC (Receiver Operating Characteristic) curve [11, 12]. The ROC shows the GAR (Genuine Accept Rate (= 100 - FRR (%))) in terms of the various FAR (False Accept Rates). As shown in Figure 12, authentication (verifi-

cation) with the proposed method showed better performance compared to other methods.

In next experiments, we measured the authentication accuracies according to the kinds of fingers. Experimental results showed that the authentication accuracies of four fingers excluding thumb were almost the same; and the authentication accuracies of the right hand fingers were almost the same as those of the left hand, too. As mentioned before, because the thumb is too short to be used with our capturing device, and the thumb is also difficult to use in the other commercial systems [15], we excluded the two thumbs for collecting our database.

4 CONCLUSION

In this paper, we have proposed a novel finger vein recognition algorithm. We made our proposed algorithm robust against irregular shading and saturation factors by using the local and global features. As a result, the EER was 0.011 % and the entire processing time was 98.2 ms.

In future work, we plan to pre-align the finger vein image based on the detected finger vein region and minutia points such as bifurcation and ending points of finger vein lines. We also plan to increase the dataset including more various ages, genders and occupations.

REFERENCES

- [1] YANAGAWA, T. et al.: Human Finger Vein Images Are Diverse and Its Patterns Are Useful for Personal Identification. *MHF 2007-12*, 2007, pp. 1–7.
- [2] MIURA, N. et al.: Feature Extraction of Finger-Vein Patterns Based on Repeated Line Tracking and its Application to Personal Identification. *Machine Vision and Applications*, Vol. 15, 2004, pp. 194–203.
- [3] ZHANG, Z. et al.: Multiscale Feature Extraction of Finger-Vein Patterns Based on Curvelets and Local Interconnection Structure. *Neural Network, The 18th International Conference on Pattern Recognition (ICPR '06)*, 2006, pp. 145–148.
- [4] MIURA, N. et al.: Extraction of Finger-Vein Patterns Using Maximum Curvature Points in Image Profiles. *IEICE Trans. Inf. & Syst.*, Vol. E90-D, 2007, No. 8, pp. 1185–1194.
- [5] ZHANG, L. et al.: Face Detection Based on Multi-Block LBP Representation. *ICB 2007, LNCS 4642*, 2007, pp. 11–18.
- [6] RODRIGUEZ, Y. et al.: Face Authentication Using Adapted Local Binary Pattern Histograms. *ECCV 2006, LNCS, Springer*, Vol. 3954, 2006, pp. IV 321–332.
- [7] DAUGMAN, J. G.: How Iris Recognition Works. *IEEE Trans. on Circuits and Systems for Video Technology*, Vol. 14, 2004, No. 1, pp. 21–29.
- [8] OJALA, T. et al.: A Comparative Study of Texture Measures With Classification Based on Feature Distributions. *Pattern Recognition* 29, 1996, pp. 51–59.

- [9] KANG, B. J. et al.: Real-Time Image Restoration for Iris Recognition Systems. *IEEE Transactions on Systems, Man and Cybernetics – Part B*, Vol. 37, 2007, No. 6, pp. 1–13.
- [10] MACMILLAN, N. et al.: *Detection Theory: A Users Guide*. New York: Cambridge University Press 1991.
- [11] MANSFIELD et al.: *Best Practices in Testing and Reporting Performance of Biometric Devices*. UK Government Biometrics Working Group, 2002.
- [12] WAYMAN, J.: *Technical Testing and Evaluation of Biometric Identification Devices*. In Jain, A. et al. (Eds.): *Biometrics: Personal Identification in Networked Society* 1999.
- [13] <http://www.fujitsu.com/global/about/rd/200506palm-vein.html> (accessed on 2010-12-27).
- [14] <http://www.tech-sphere.com> (accessed on 2010-12-27).
- [15] <http://www.hitachi.com/products/business/security.html> (accessed on 2010-12-27).
- [16] SUN, Z. et al.: Graph Matching Iris Image Blocks with Local Binary Pattern. *ICB* 2006, Vol. 3832, 2006, pp. 366–372.
- [17] <http://www.adobe.com/products/photoshop/index.html> (accessed on 2010-12-27).
- [18] JANG, Y. K.—KANG, B. J.—PARK, K. R.: A Study on Touchless Finger Vein Recognition Robust to the Alignment and Rotation of Finger. *Journal of Korea Information Processing Society*, Vol. 15-B, August 2008, No. 4, pp. 275–284.
- [19] SEMLER, L.—DETTORI, L.—FURST, J.: Wavelet-Based Texture Classification of Tissues in Computed Tomography. *Proceedings of 18th IEEE Symposium on Computer-Based Medical Systems*, 2005, pp. 265–270.
- [20] GONZALEZ, R. C.—WOODS, R. E.: *Digital Image Processing*. 2/E, Prentice Hall 2002.
- [21] DRUCKER, H.—BURGES, C.—KAUFMAN, L.—SMOLA, A.—VAPNIK, V.: Support Vector Regression Machines. *Advances in Neural Information Processing Systems*, Vol. 9, 1996, pp. 155–161.
- [22] SCHOLKOPF, B.—WILLIAMSON, R. C.—SMOLA, A. J.—SHAWE-TAYLOR, J.: In: Solla, S., Leen, T., Muller, K.-R. (Eds.): *Neural Information Systems*, Vol. 12, MIT Press, USA 2000.



Park Kang Ryoung received his B.Sc. and M.Sc. degrees in Electronic Engineering from Yonsei University, Seoul, Korea, in 1994 and 1996, respectively. He also received his Ph.D. degree in Electrical and Computer Engineering, Yonsei University, in 2000. He was an Assistant Professor in the Division of Digital Media Technology at Sangmyung University from March 2003 to February 2008. He has been an Assistant and Associate Professor in the Division of Electronics and Electrical Engineering at Dongguk University since March 2008. His research interests include computer vision, image processing, and biometrics.